Journal of Aeronautics, Astronautics and Aviation, Vol.49, No.1, pp.013 - 022(2017)
*DOI: 10.6125/*16-1014-907

An Adaptive Sampling VB-IMM based on ADS-B for TCAS Data Fusion with Benefit Analysis *

Zhou Yun Dai[1], Gang Xiao[1 **], Du Yu Liu[1], Fang He[1] and Jin Hua Xie[2]

[1]*School of Aeronautics and Astronautics, Shanghai Jiao Tong University, Dongchuan Road, 200240, Shanghai, China*
[2]*AVIC Radar and Avionics Institute, 214063, Wuxi, Jiangsu, China*

ABSTRACT

This paper discusses the problem of data fusion of Automatic Dependent Surveillance Broadcast and Traffic Alert and Collision Avoidance System. First, the 3-dimensional trajectory is generated by aircraft movement model. Contrasting to traditional aircraft surveillance research focusing on data precision with known noise and fixed sampling period, the estimation of time-varying noise is guaranteed by Variational Bayesian method, which is the basis for failure prediction and adjustment of sampling period. Second, the interacting multiple model is used for local filtering. Two situations are considered during fusion, including scenarios before and after injecting Automatic Dependent Surveillance Broadcast failure modes. Then, data fusion's benefit for improving the false alarm and leak alarm is analyzed by calculating the time until closest point of approach between aircraft. Finally, simulations results are given to verify the validity of the algorithm proposed in this paper. It shows that the dynamic noise can be estimated within a tolerable error range and the sampling period can be adjusted according to the noise level. Compared to single Traffic Alert and Collision Avoidance System, Automatic Dependent Surveillance Broadcast system and current statistical model based fusion system, the root mean squared error, alarm condition can be optimized and failure at information level can be detected.

Keywords: variable sampling period VB-IMM, data fusion, ADS-B failure mode, benefit analysis

I. INTRODUCTION

The problem of position estimation of aircraft within airspace is known as target tracking, which is a fundamental requirement for surveillance systems. TCAS is known as Traffic Alert and Collision Avoidance System. It interrogates nearby aircraft equipped with TCAS through Mode S data link, processes returned data and displays potential dangerous targets. Automatic Dependent Surveillance Broadcast (ADS-B) is an important part of the Future Air Navigation System (FANS). It is designed to provide air traffic avoidance and management especially in remote areas, complex terrain and ocean areas. TCAS sends interrogation signal with the frequency of 1030 MHz and receives a signal from another transponder with the frequency of 1090 MHz. ADS-B broadcasts information with the frequency of 1090 MHz as well. ADS-B's integrity category, integrity level and navigation accuracy of surveillance information depend on the performance of GNSS. If ADS-B is utilized only, GNSS information's loss caused by interferences or other factors will lead to catastrophic consequences. The above-mentioned issues put forward the demand for research of TCAS and ADS-B's fusion, which can lay the foundation of airspace interval compression, flight path optimization [1] and coordination avoidance among manned, unmanned aerial vehicles and general aviation aircraft.

* Manuscript received, October 14, 2016, final revision, December 26, 2016
** To whom correspondence should be addressed, E-mail: xiaogang@sjtu.edu.cn

Julio L. R. da Silva applied data fusion techniques to ADS-B and Radar Sensors with Kalman Filter [2]. Gui Ping He [3], Yun Song Lin [4] studied ADS-B and TCAS hybrid surveillance. They focused on data precision through x-y trajectory, and current statistical (CS) model is the foundation. But it is not appropriate for civil aircraft when in cruise. Roberto Sabatini and Robert H. Chen introduced Sense-and-Avoid (SAA) system [5, 6]. Extended Kalman Filter and common interacting multiple model (IMM) [7] algorithm were used to estimate the intruder's state vector. Federal Aviation Administration (FAA) and Thales Company focused on the IMM tracking models. They designed the Constant Velocity (CV), Constant Acceleration (CA) and Constant Turning (CT) models for the surface tracking [8], and finally took IMM to improve precision. IMM is one of the most cost-effective schemes for targets with multiple kinematic behaviors. But most methods are based on the assumption of a priori knowledge of measurements and dynamic model parameters, including the noise statistics, which is not practical. Roxaneh Chamlou [9] put forward the layout of future studies about TCAS, ADS-B fusion and performance evaluation. The concept of noise parameters was mentioned, but without research on detailed algorithms. The consideration of online estimation and adaptive adjustment of measurement noise is necessary. The classical approaches about adaptive noise filtering can be divided into Bayesian, maximum likelihood, correlation and covariance matching methods. Variational Bayesian (VB) method [10] has been developed for a wide range of models to perform approximate posterior inference at low computational cost and adapts quickly in a large scope compared with the sampling methods. Simo Sarkk's VB method [11] approximated the joint posterior distribution of the state and the noise variance by a factorized free form distribution, where on each step the sufficient statistics are estimated with a fixed-point iteration of Kalman filter. The forgetting factor ρ is a constant in this method. ρ=1 corresponds to stationary variance and a smaller value corresponds to a stronger assumed time-fluctuation.

Therefore, the factor ρ's dynamic adjustment and CS model based Kalman filter are introduced in the VB estimation in this paper. Meantime, the sampling period of VB-IMM is adjusted adaptively according to fluctuation of noise variance. In addition, Busyairah Syd Ali [12] analyzed and listed ADS-B system's failure modes. There is few research about benefit analysis of fusion system after failures injected [13]. This paper conducts benefit analysis about alarm condition, and is organized as follows: Section II presents mathematical formulations used for variable sampling VB-IMM (VSVB-IMM). Section III compares the tracking performance and alarm condition of CS model algorithm, fixed sampling VB-IMM (FSVB-IMM) and VSVB-IMM. Conclusions are presented in IV.

II. COMPUTATIONAL METHOD

2.1 Markov jump linear system and tracking model

The target dynamics are modeled in Cartesian coordinate system. The Markov jump linear system [14]:

$$X(k+1)=\Phi_j(k)X(k)+\omega_j(k) \tag{1}$$

$$z(k)=H_jX(k)+\upsilon_j(k) \tag{2}$$

where the state $X(k)$ is an n-dimensional vector, the observation z(k) is an m-dimensional vector and the subscript $j\in S=\{1,\ 2,\ \ldots,\ s\}$ denotes the models. The matrix functions $\Phi(k),\Gamma(k),H$ are known. The variable $\omega_j(k)$ is a zero-mean white Gaussian process noise with known variance:

$$E[\omega_j(k)]=0,\ E[\omega_j(t)\omega_j(k)^T]=Q_j\delta(t,k) \tag{3}$$

$\delta(t,k)$ is the Kronecker delta function. The variable $\upsilon_j(k)$ is an independent Gaussian measurement noise with zero-mean and variance to be estimated:

$$E[\upsilon_j(k)]=0,\ E[\upsilon_j(t)\upsilon_j(k)^T]=R_j\delta(t,k) \tag{4}$$

M_j^k denotes the flight model j at time k. The model dynamics are modeled as a finite Markov chain with known model-transition probabilities from model i at time k-1 to model j at time k:

$$\pi_{ij}=\text{Prob}\{M_j^k\mid M_i^{k-1}\}=P\{M_j^k\mid M_i^{k-1}\} \tag{5}$$

where $0\le\pi_{ij}\le 1,\sum_{j=1}^{s}\pi_{ij}=1,i,\ j\in S$.

The initial state distribution of the Markov chain is $\varphi=[\varphi_1,\ldots\varphi_s]$, where $0\le\varphi_j\le 1,\sum_{j=1}^{s}\varphi_j=1,\ j\in S$.

The model set S describes the target motion states. CV, CA and CS are typical models. The IMM algorithm in this paper includes the above three models. The longitude, latitude, and altitude are processed separately. $X(k)$ is the target state at time k. It can be a 3-dimensional vector consisting of position, velocity and acceleration in each direction.

Model 1: CV model for non-maneuvering flight segments is described in equation (6), T is the sampling period.

$$X(k)=[x\ \dot{x}\ \ddot{x}],\Phi(k)=\begin{bmatrix}1 & T & 0\\ 0 & 1 & 0\\ 0 & 0 & 0\end{bmatrix} \tag{6}$$

Model 2: CA model for maneuvering flight segments with the following transition matrix (7):

$$\Phi(k)=\begin{bmatrix}1 & T & T^2/2\\ 0 & 1 & T\\ 0 & 0 & 1\end{bmatrix} \tag{7}$$

Based on CA and singer model, Hong Ren Zhou [15] proposed CS model and pointed out that the noise of maneuvering target acceleration should be corrected with Rayleigh distribution. The acceleration is assumed as non-zero and finite in the neighborhood of current acceleration. The model is described in equation (8-12).

Model 3: Current statistical model:

$$X(k+1)=\Phi_j(k)X(k)+\Gamma_j(k)\bar{a}+\omega_j(k) \tag{8}$$

$$z(k)=H_jX(k)+\upsilon_j(k) \tag{9}$$

$$\Phi(k)=\begin{bmatrix}1 & T & (-1+\alpha T+e^{-\alpha T})/\alpha^2\\ 0 & 1 & (1-e^{-\alpha T})/\alpha\\ 0 & 0 & e^{-\alpha T}\end{bmatrix},\Gamma(k)=\begin{bmatrix}(-T+\alpha T^2/2+(1-e^{-\alpha T})/\alpha)/\alpha\\ T-(1-e^{-\alpha T})/\alpha\\ 1-e^{-\alpha T}\end{bmatrix} \quad (10)$$

where $\omega_j(k)$, $\upsilon_j(k)$ are zero-mean, independent Gaussian white noise. $\Phi_j(k)$ is state transition matrix. $\Gamma_j(k)$ is input matrix. T is sampling period. α is maneuvering frequency.

The process noise matrix $\mathrm{Q(k)}=2\alpha\sigma_a{}^2\mathrm{Q}$, Q is a matrix containing variable period T. $\sigma_a{}^2$ is the maneuvering acceleration variance.

$$Q=\begin{bmatrix}q_{11} & q_{12} & q_{13}\\ q_{12} & q_{22} & q_{23}\\ q_{13} & q_{23} & q_{33}\end{bmatrix} \quad (11)$$

The most common treatment for maneuvering acceleration variance:

$$\begin{cases}\sigma_a{}^2=\dfrac{4-\pi}{\pi}(\mathrm{a_{max}}-\hat{a}(\mathrm{k}\,|\,\mathrm{k}-1)),\ if\ \ \mathrm{a}\ge 0\\ \sigma_a{}^2=\dfrac{4-\pi}{\pi}\left(\hat{a}\left(\mathrm{k}|\mathrm{k}-1\right)-\mathrm{a_{-max}}\right),\ f\ \ \mathrm{a}<0\end{cases} \quad (12)$$

where $\mathrm{a_{max}}$, $\mathrm{a_{-max}}$ are upper and lower bounds of acceleration, $\hat{a}(\mathrm{k}\,|\,\mathrm{k}-1)$ is the acceleration estimation.

In the filtering, $\hat{X}(k+1/k+1)$ is obtained by

$$\hat{X}(k+1/k+1)=\hat{X}(k+1/k)+K(k+1)[Z(k+1)-H(K+1)\hat{X}(k+1/k)] \quad (13)$$

$$K(k+1)=[F(k)P(k/k)F(k)^T+Q(k)]H(k+1)^T*[H(k+1)P(k+1/k)H(k+1)^T+R(k+1)]^{-1} \quad (14)$$

where $K(k+1)$ is a gain matrix. From equation (13, 14) we can draw the conclusion that the adjustment of $Q(k)$ or $R(k+1)$ can improve the accuracy of estimation.

Binbin Li [16] used Gaussian membership function of fuzzy control theory to improve the CS model. It sets $\mathrm{f(x,y,\sigma)}=1-e^{-\frac{(x-y)^2}{\mu\sigma^2}}$, where x, y, σ^2 and μ are the position's input, the current position's estimation, the variance of innovation and a constant respectively. The value $|x-y|$ is larger when there is a larger maneuvering, then $\mathrm{f(x,y,\sigma)}\to 1$.The system tracks with a larger variance. On the contrary, the system tracks with a smaller variance, $\mathrm{f(x,y,\sigma)}\to 0$, $\mathrm{Q(k)}=2\mathrm{a}\sigma_a{}^2\mathrm{Q}*\mathrm{f(x,y,\sigma)}$.

2.2 VB-IMM algorithm

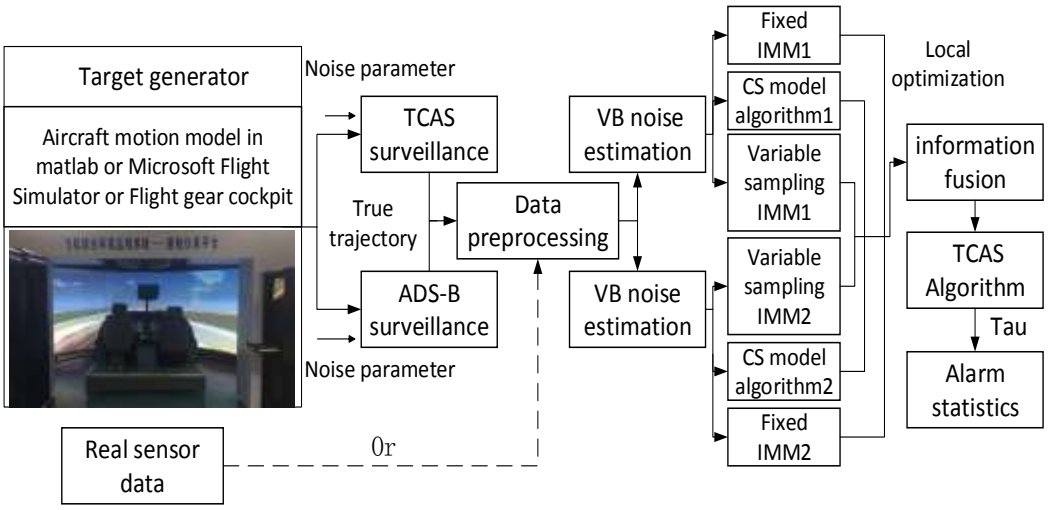

Figure 1 System frame diagram

In this section, a brief review of the IMM algorithm for maneuvering target tracking is given, and the VB approximation is applied to estimate unknown noise variance. The IMM algorithm runs CV, CA and CS model filters in parallel. The state is obtained by a weighted sum of the estimates from all filters with different motion models. The local optimized value is obtained through variable sampling IMM (VSIMM), fixed sampling IMM (FSIMM), CS model algorithm based on the TCAS, ADS-B data and VB noise estimation. The global optimal value is achieved under the optimal information fusion criterion. The results from three different algorithms will be used as inputs of TCAS logic and then the time until closest point of approach (tau) is calculated. Finally, false alarm and leak alarm are counted for statistical analysis.

Firstly, ADS-B Latency should be considered in the data preprocessing. Busyairah Syd Ali [17] developed a comprehensive framework to evaluate ADS-B performance using the London Terminal Maneuvering Area (LTMA) as a case study. It introduced the ADS-B latency model, which incorporates delay in the navigation system (Δa), delay within the interfacing between the navigation system and the ADS-B emitter (Δb), delay in the ADS-B emitter (Δc), propagation delay (Δd), and delay in other aircraft or ground station (Δe). The results show that 66.7% of the aircraft's latency is less than one second.

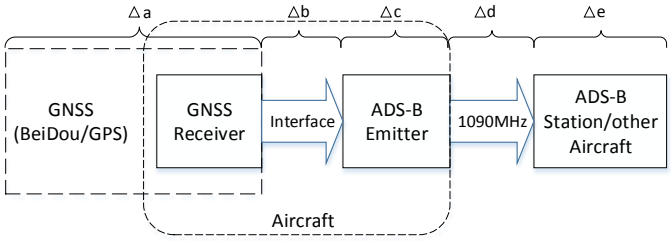

Figure 2 ADS-B latency model

The aircraft clocks can be calibrated by GPS satellites which use atomic clocks. Therefore the TCAS and ADS-B data can both be time stamped. The time synchronization in TCAS and ADS-B data fusion proposed by Yude NI [18] is improved. In a unified coordinate system, ADS-B data is obtained based on TCAS's time:

$$k = \left[\frac{t_{TCAS} - t_{ADS-B}}{\Delta T} \right], k \in N^+ \tag{15}$$

$$Z_{ADS-B}(t_{TCAS}) = Z_{ADS-B}(t_{ADS-B}) + \sum_{i=1}^{k} v_i \cdot \Delta T + v_{i+1}(t_{TCAS} - t_{ADS-B} - k \cdot \Delta T) \tag{16}$$

Where t_{TCAS} , t_{ADS-B} are the time stamp of TCAS and ADS-B data. ΔT is the interval of aircraft speed's intensive sampling. v_i is the speed in sampling point. $Z_{ADS-B}(t_{TCAS})$ is the extrapolated ADS-B data. If $t_{TCAS} - t_{ADS-B}$ is bigger than 2 seconds. The ADS-B data in that moment will be ignored and only TCAS data will be used in collision avoidance logic. But the probability is very low.

Then, the formal algorithm flow starts. The unknown measuring noise variance is estimated by VB algorithm [19], which is described by equation (17-25). $\rho_i \in (0,1]$ is a forgetting factor and is sensitive to the convergence of noise estimation. It should be related to the fluctuation and amplitude of the noise variance in the previous step. Inspired by Gaussian membership function, the following equation (17) is defined. c_1, c_2, c_3 are constants, c_3 maintains the stability, c_1 represents the effect of variance in the previous step, c_2 represents the effect of variance fluctuation. $m_{k-1}(3,1)$ is acceleration estimation.

Step 1. Parameters of predicted distribution

$$\rho_i = e^{\frac{c_1\sigma_i(k-1)+c_2(\sigma_i(k-1)-\sigma_i(k-2))^2+c_3}{100000}} \tag{17}$$

$$m_k^- = \Phi(k) m_{k-1} + \Gamma(k) m_{k-1}(3,1) \tag{18}$$

$$P_k^- = \Phi(k) P_{k-1} \Phi(k)^T + Q_k \tag{19}$$

$$\alpha_{k,i}^- = \rho_i \alpha_{k-1,i}, i = 1,...,d \tag{20}$$

$$\beta_{k,i}^- = \rho_i \beta_{k-1,i}, i = 1,...,d \tag{21}$$

Step 2. Update

Set $m_k^0 = m_k^-, P_k^0 = P_k^-, \alpha_{k,i} = 1/2 + \alpha_{k,i}^-, \beta_{k,i}^{(0)} = \beta_{k,i}^-, i = 1,...,d$, d is the dimension of measurement vector. Then iterate the following equations for N steps:

$$\sigma_k^{(n)} = diag(\beta_{k,1}^{(n)} / \alpha_{k,1}^{(n)}, ..., \beta_{k,d}^{(n)} / \alpha_{k,d}^{(n)}) \tag{22}$$

$$m_k^{(n+1)} = m_k^- + P_k^- H_k^T (H_k P_k^- H_k^T + \sigma_k^{(n)})^{-1} (y_k - H_k m_k^-) \tag{23}$$

$$P_k^{(n+1)} = P_k^- - P_k^- H_k^T (H_k P_k^- H_k^T + \sigma_k^{(n)})^{-1} H_k P_k^- \tag{24}$$

$$\beta_{k,i}^{(n+1)} = \beta_{k,i}^- + \frac{1}{2}(y_k - H_k m_k^{(n+1)})_i^2 + \frac{1}{2}(H_k P_k^{(n+1)} H_k^T)_{ii} \tag{25}$$

and set $\beta_{k,i} = \beta_{k,i}^{(N)}, m_k = m_k^{(N)}, P_k = P_k^{(N)}$.

The above estimated noise variance is used for IMM filtering [20], which is shown in equation (26-36).

Notations: p_{ij} is transition matrix. $\hat{x}_j(k|k)$, $P_j(k|k)$ are the state estimation and covariance in mode-matched filter j at time k. $\hat{x}_{0j}(k|k)$, $P_{0j}(k|k)$ are the mixed initial condition for mode-matched filter j at time k. $\hat{x}(k|k)$, $P(k|k)$ are the combined state estimation and covariance. $\mu_j(k)$ is the mode probability at time k. $\mu_{i|j}(k|k)$ is the mixing probability at time k. $\Lambda_j(k)$ is the likelihood function of filter j. $\sigma_j(k) = \sigma_k^N$ is the estimation of measurement noise variance by VB algorithm.

Step 3. Calculation of mixing probabilities

$\forall i, j \in M_s$, $\bar{c}_j$ is a normalization factor.

$$\mu_{i|j}(k-1|k-1) = (1/\bar{c}_j) p_{ij} \mu_i(k-1), \bar{c}_j = \sum_i p_{ij} \mu_i(k-1) \tag{26}$$

Step 4. Interaction

The mixed system state estimation is given by

$$\hat{x}_{0j}(k-1|k-1) = \sum_i \hat{x}_i(k-1|k-1) \mu_{i|j}(k-1|k-1) \tag{27}$$

$$P_{0j}(k-1|k-1) = \sum_i \{P_i(k-1|k-1) + [\hat{x}_i(k-1|k-1) - \hat{x}_{0j}(k-1|k-1)] \times [\hat{x}_i(k-1|k-1) - \hat{x}_{0j}(k-1|k-1)]^T\} \mu_{i|j}(k-1|k-1) \tag{28}$$

Step 5. Filtering

$\forall j \in M_s$, the measurement noise variance is obtained by VB estimation rather than a predetermined constant in the common IMM algorithm. The state estimation and covariance matrix is obtained by running each filter:

$$\hat{x}_j(k|k-1) = \Phi_j(k-1) \hat{x}_{0j}(k-1|k-1) + \Gamma_j(k-1) \hat{a}_j(k-1) \tag{29}$$

where $\begin{cases} \hat{a}_j(k-1) \neq 0, \text{ if } CS \text{ model} \\ \hat{a}_j(k-1) = 0, \text{ if } CV, CA \text{ model} \end{cases}$.

$$r_j(k) = z(k) - z_j(k|k-1) \quad \text{(residual)} \tag{30}$$

$$z_j(k|k-1) = H_j(k) \hat{x}_j(k|k-1) \quad \text{(prediction)} \tag{31}$$

$$S_j(k) = H_j(k) P_j(k|k-1) H_j(k)^T + \sigma_j(k) \quad \text{(covariance)} \tag{32}$$

$$K_j(k) = P_j(k|k-1) H_j(k)^T S_j(k)^{-1} \quad \text{(filter gain)} \tag{33}$$

$$P_j(k|k-1) = \Phi_j(k-1) P_{0j}(k-1|k-1) \Phi_j(k-1)^T + \Gamma_j(k-1) \times Q_j(k-1) \Gamma_j(k-1)^T \tag{34}$$

$$\hat{x}_j(k|k) = \hat{x}_j(k|k-1) + K_j(k) r_j(k) \tag{35}$$

$$P_j(k|k) = P_j(k|k-1) - K_j(k) S_j(k) K_j(k)^T \tag{36}$$

Step 6. Calculation of likelihood function

The likelihood function is calculated by the residual measurement and covariance, d is the dimension of measurement vector.

$$\Lambda_j(k) = N(r_j(k):0, S_j(k)) = \frac{1}{(2\pi)^{d/2}\left|S_j(k)\right|^{1/2}} \exp(-\frac{1}{2} r_j(k)^T S_j(k)^{-1} r_j(k)) \quad (37)$$

$$\mu_j(k) = \frac{1}{c}\Lambda_j(k)\bar{c}_j, c = \sum_{j=1}^{s}\Lambda_j(k)\bar{c}_j \quad (38)$$

Step 7. Combination of state estimation and covariance

$\hat{x}(k|k)$, $\hat{P}(k|k)$ are estimated by a weighted sum of the estimations from all filters, $\forall i, j \in M_s$

$$\hat{x}(k|k) = \sum_j \hat{x}_j(k|k)\mu_j(k) \quad (39)$$

$$P(k|k) = \sum_j \{P_j(k|k) + [\hat{x}_j(k|k) - \hat{x}(k|k)]\times [\hat{x}_j(k|k) - \hat{x}(k|k)]^T\}\mu_j(k) \quad (40)$$

2.3 Variable sampling period VB-IMM and fusion

Variable sampling period [21]: FAA issued advisory circular about Airworthiness Approval of ADS-B Out Systems in 2010 [22]. The concept of Navigation Accuracy Category for Position (NAC_P) specifies the accuracy of the aircraft's horizontal position information (latitude and longitude) transmitted from the aircraft avionics. The ADS-B equipment derives a NAC_P value from the position source's accuracy output, such as the HFOM from the GNSS. The NAC_P specifies with 95% probability that the reported information is correct within an associated allowance.

The sampling period can increase appropriately when estimated variance by VB algorithm is relatively small. So the simulation sampling period is 1s in the NAC_P 10 and 11 in Table 1. The sampling should be intensive when the estimated variance increases and meantime the intruder is closer. The sampling period in simulation is 0.8s in the NAC_P 9 and 0.6s in the NAC_P 8, 7, 6. When the intruder is far away, sampling period is restored to 1s. EPU is Estimated Position Uncertainty.

Table 1 NAC_P Values

NAC_P	Horizontal Accuracy Bound	Simulation sampling period
0	EPU ≥ 18.52 km (10nm)	1s
1	EPU < 18.52 km (10nm)	1s
2	EPU < 7.408 km (4nm)	1s
3	EPU < 7.408 km (4nm)	1s
4	EPU < 1852 m (1nm)	1s
5	EPU < 926 m (0.5nm)	0.8s
6	EPU < 926 m (0.5nm)	0.6s
7	EPU < 185.2 m (0.1nm)	0.6s
8	EPU < 92.6 m (0.05nm)	0.6s
9	EPU < 30 m	0.8s
10	EPU < 10 m	1s
11	EPU < 3 m	1s

Optimal Information Fusion Criterion [23]: There are unbiased estimations of L sensors, $\hat{x}_i, i = 1,\ldots,L$. The estimation error covariance matrix $P_{ij}, i, j = 1,\ldots L$ is obtained. The fusion is performed according to matrix weighted linear minimum variance criterion, $\hat{x}_0 = \sum_{i=1}^{L} A_i \hat{x}_i$, where $[A_1,\ldots,A_L] = \left(e^T P^{-1} e\right)^{-1} e^T P^{-1}$, A_i is an n-order square matrix, P is a block matrix with P_{ij} as the (i, j) element. I_n is an n-order identity matrix, $e = [I_n \ \cdots \ I_n]^T$. The optimal fusion estimation of error covariance matrix is $P_0 = \left(e^T P^{-1} e\right)^{-1}$. In this paper, L=2. Fusion equations:

$$[A_{TCAS}, A_{ADS-B}] = [A_1, A_2] = \left(e^T P^{-1} e\right)^{-1} e^T P^{-1} \quad (41)$$

$$\hat{X}_f = A_1\hat{x}_1 + A_2\hat{x}_2 = A_{TCAS}\hat{x}_{TCAS} + A_{ADS-B}\hat{x}_{ADS-B} \quad (42)$$

where $P = \begin{bmatrix} P_{11} & P_{12} \\ P_{21} & P_{22} \end{bmatrix}, P_{ij} = \mathrm{cov}(\hat{x}_i, \hat{x}_j), i, j = 1,2, e = [I_3 \ I_3]^T$.

$\hat{x}_{TCAS}$, $\hat{x}_{ADS-B}$ are obtained from the results of variable sampling VB-IMM, fixed sampling VB-IMM and CS model algorithm.

III. RESULTS AND DISCUSSION

3.1 Experimental setup

The 3-dimensional trajectory can be generated by aircraft motion model, Microsoft Flight Simulator or Flight gear cockpit shown in figure 1. The real TCAS measurements are height, azimuth and distance. The position estimation error of intruders includes the position error of own aircraft and the measurement error of TCAS. In order to facilitate modeling and simulation, unified conversion is conducted to express as latitude, longitude and height with different noises. The estimation accuracy of VSVB-IMM, FSVB-IMM, CS model algorithm are analyzed. It is essential to calculate tau combining the core processing model of TCAS. Then statistics of false alarm, leak alarm and benefit analysis for fusion system were conducted.

The simulation parameters are set as follows: Flight experience is 3000s, fixed sampling period T=1s, the variable sampling period is adaptive. Own flight position: 29°00'00"N, 103°12'00"E, 4800m height. Intruder's initial position: 29 °00'00"N, 106 °00'00"E, 300m height. TCAS's observation noise standard deviation is 50 m/s, ADS-B's observation noise standard deviation is time-varying. The aircraft climbs gradually from 300m, then cruises at constant height.

3.2 Flight parameter estimation and IMM probability transformation

The aircraft maneuvers during step 12500 and step 12650, Figure 3 shows the acceleration's true value and estimation from different directions of the aircraft by VSVB-IMM and FSVB-IMM.

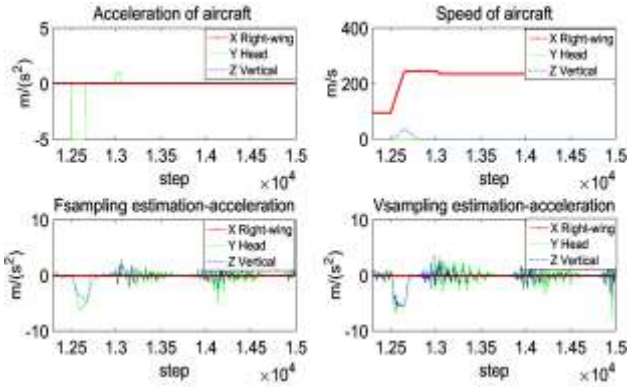

Figure 3 Estimation of aircraft motion parameters

Figure 4 is the model probability transformation. The mode 1 is CV, mode 2 is CA, mode 3 is CS model. The maneuver occurs between step 12500 and 12650 in the nose direction (longitude direction). The CS and CV probability increase rapidly in the longitude direction and CV probability drops. The CA model is dominant later because the main form of motion is CA in this interval. Another maneuver occurs at step 13000.

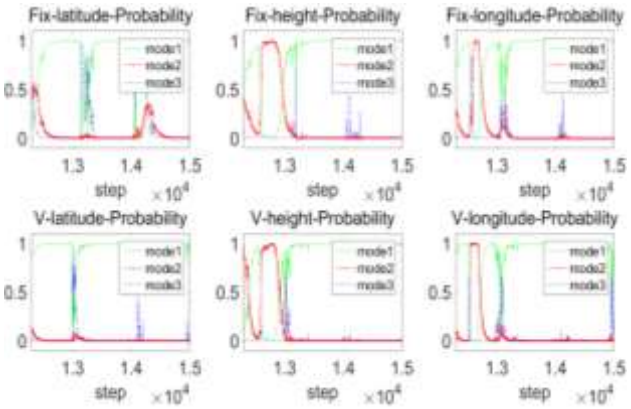

Figure 4 IMM probability transformation

3.3 Sampling period and tau calculation based on TCAS model

Figure 5 is the result distribution of adaptive sampling period. The red line is the period of FSIMM and green line is the period of VSIMM, which is adjusted mainly between 3s and 6s.

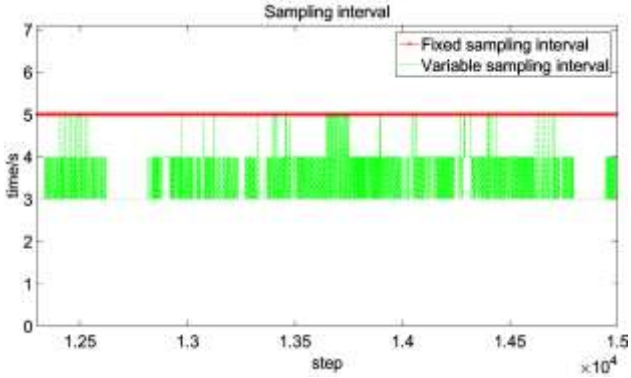

Figure 5 Sampling period superimposed distribution

After geodetic and Earth-Centered Earth-Fixed coordinate conversion, the local trajectory is filtered by VSVB-IMM and the fusion results are given as inputs to TCAS logic. The relative position of aircraft is calculated and the time until closest point of approach is estimated based on trend extrapolation method. It is vital to anticipate conflict and make RA decision based on tau. Figure 6 is the result of tau calculation by different systems, which includes true value in blue line. It's the superimposed distribution after 60 Monte Carlo experiments.

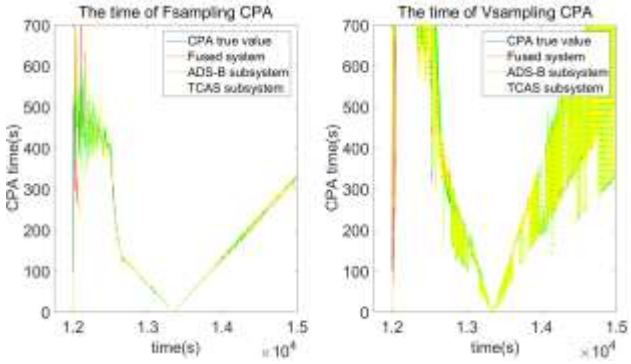

Figure 6 Tau of each system

3.4 Noise estimation by Variational Bayesian

In the simulation, TCAS contains fixed noise, whose amplitude of standard deviation is 50 m/s. The oscillatory behavior may result from the modeling of dynamics, reaction effect of initial conditions and calibration errors. And the sinusoidal oscillation noise is injected into ADS-B system. Its amplitude of standard deviation is 40 m/s. Figure 7 and Figure 8 are the online variance estimation of measurement noise. The green line represents the true value and red line represents the estimation. Forgetting factor is a sensitive parameter for VB. It is adaptive as described in 2.2. The number of iteration N in each cycle is 30 in this paper. Although there are some deviations and hysteresis of estimated noise, IMM can run normally in the range of acceptable root mean squared error (RMSE).

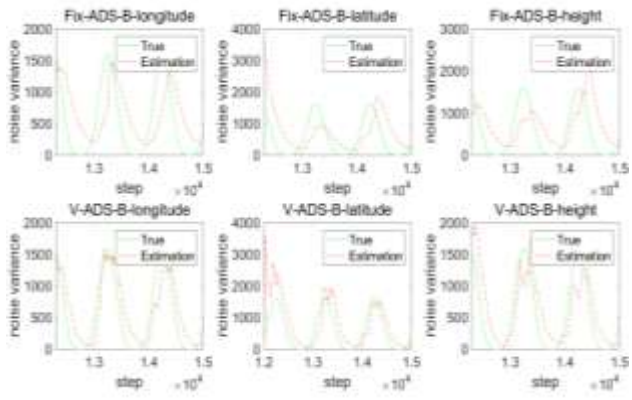

Figure 7 Noise estimation of ADS-B

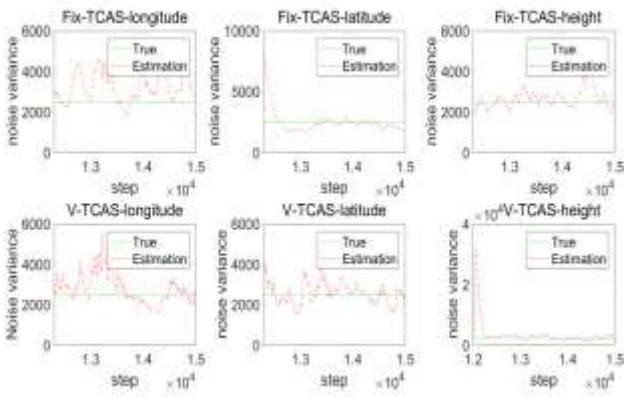

Figure 8 Noise estimation of TCAS

3.5 Statistics of root mean squared error

The RMSE is calculated according to

$$RMSE_{\mathrm{k}} = [\frac{1}{M}\sum_{i}^{M}(x_k^{(i)} - \hat{x}_k^{(i)})^2]^{\frac{1}{2}}, k = 1, 2...step \quad (43)$$

where M is the number of Monte Carlo, k is the steps of simulation. Figure 9 is the statistical result of 60 Monte Carlo experiments. The RMSE of fusion system is smaller than TCAS and ADS-B subsystem. The VSVB-IMM is superior to FSVB-IMM as purple line with triangles is the smallest most of the time. The same conclusion can be drawn from the numerical result in Table 2.

3.6 False alarm, leak alarm analysis

The number of false alarm and leak alarm during the TA (tau in 35-45s) and RA (tau<35s) interval is analyzed. The false alarm is defined that the estimated tau is smaller than theory alarm time in sampling point and exceeds the threshold (can be set to a constant 1s). Leak alarm is defined that the estimated tau is bigger than theory alarm time in sampling point and exceeds the threshold (1s). In Table 2, from the horizontal comparisons of the same sampling conditions, like first three columns and last three columns, or vertical comparisons from different sampling conditions, like column 2,5, column 3,6. We can draw the conclusion that fusion can reduce the incidence of false alarm, leak alarm in the TA and RA interval. Leak alarm and delayed alarm compress avoidance response time of system and pilot, thus seriously affect flight safety. Therefore, a more accurate alarm time can improve the system security and bring forward earnings.

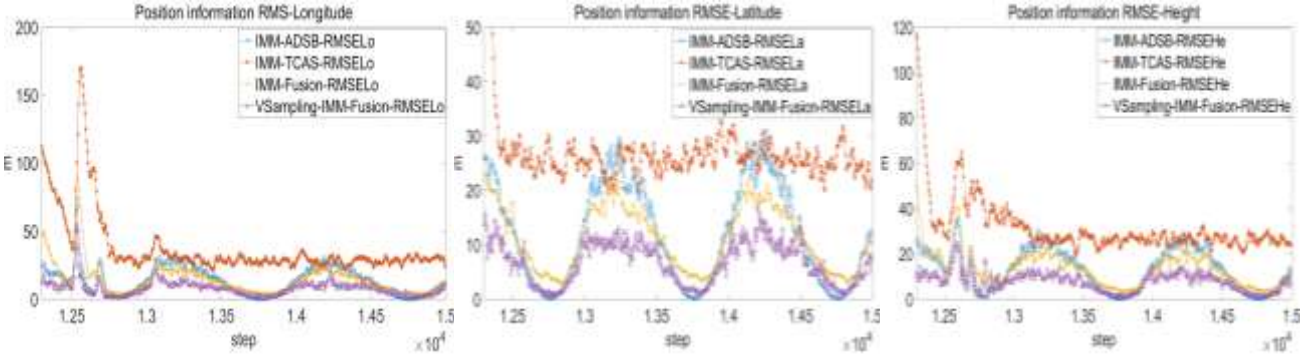

Figure 9 Root mean squared error of statistics in each direction

Table 2 Performance comparison of various algorithms

Case	*Longitude RMSE,m*	*Latitude RMSE,m*	*Height RMSE,m*	*False alarm(RA)*	*Leak alarm(RA)*	*False alarm(TA)*	*Leak alarm(TA)*
FIMM-TCAS	29.8684	26.0890	26.6773	376	330	291	302
FIMM-ADS-B	16.5508	16.3195	15.9397	198	195	185	152
FIMM-Fusion	14.2319	13.1903	13.1918	132	151	158	148
VIMM-TCAS	19.0613	17.9499	17.9382	226	189	221	173
VIMM-ADS-B	11.1504	10.3604	10.7635	165	156	158	130
VIMM-Fusion	**9.1981**	**8.3820**	**8.1759**	**73**	**72**	**123**	**88**

The unit of alarm: frequency, FIMM-TCAS: fixed sampling IMM under TCAS measurement, FIMM-ADS-B: fixed sampling IMM under ADS-B, FIMM-Fusion: fixed sampling IMM after fusion, V represents variable sampling period.

3.7 Failure mode injection and benefit analysis

Donald McCallie [24] conducted security analysis of the ADS-B implementation in the next generation air transportation system. This paper focuses on TCAS, ADS-B data fusion by VSVB-IMM and benefit analysis. The typical failure modes are injected, including data loss, step, ramp and oscillation.

The original 3-dimensional information changes into Gaussian white noise. It's a simulation about ADS-B navigation data loss. The possibility of large transition of aircraft's location, speed and acceleration does not exist. The state change before and after in the physical system is finite. When the noise estimation by VB diverges as shown in Figure 10, the trajectory RMSE diverges as well. Fusion system can locate failure [25] like data loss and aberration by detecting the noise estimation. Then it takes measures to adjust fusion weight and ensures the availability, security of the hybrid surveillance system.

Although the precision is worse than before, it may downgrade to TCAS's accuracy and false alarm, leak alarm condition. The system stability is guaranteed, and it brings positive gains. Meantime, the false alarm and leak alarm in VSVB-IMM are better than FSVB-IMM.

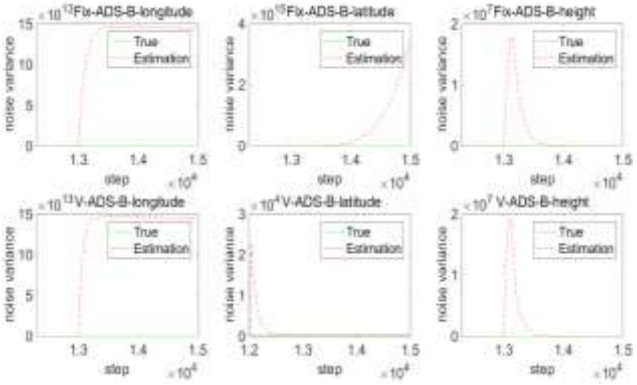

Figure 10 Noise estimation of ADS-B

Figure 11 to 14 show the system response when step and ramp failure are injected into ADS-B's information. Step mode includes an abrupt change without notification. When there are sudden jump in the signal, unavailability of the data link connection and human errors. Figure 12 proves that fusion can guarantee the system stability and alarm condition is superior to single system. Modern aircraft integrated GNSS and inertial navigation system can provide position, speed and data quality identification for ADS-B transmission. Ramp can simulate signal failure in fusion system or even serious drift of INS when GNSS is lost. In Figure 13 and 14, the ADS-B alarm condition deteriorates after ADS-B failures. But the fusion system can utilize the useful information of both TCAS and ADS-B measurements, ensure that the alarm condition is optimal compared to TCAS system and ADS-B system.

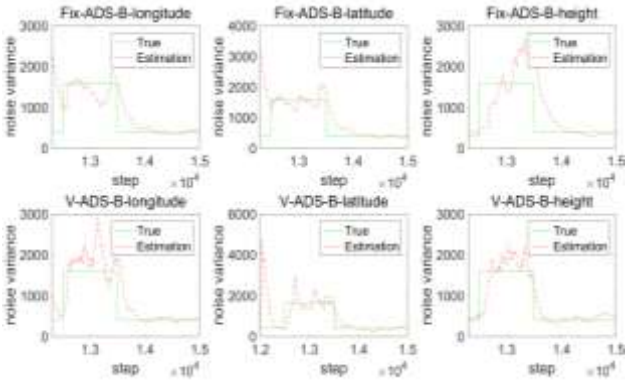

Figure 11 Noise estimation of ADS-B

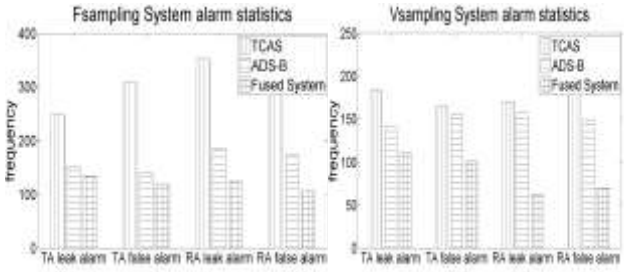

Figure 12 Statistics of false alarm, leak alarm

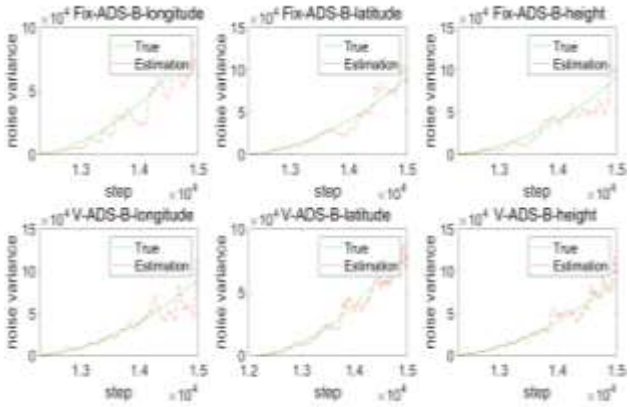

Figure 13 Noise estimation of ADS-B

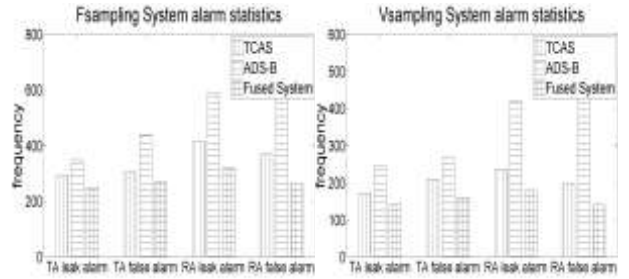

Figure 14 Statistics of false alarm, leak alarm

VI. CONCLUSION

This paper fuses 3-dimensional trajectory by VSVB-IMM. The estimated noise by VB method is the basis for failure prediction and adjustment of sampling period. It is proved that VSVB-IMM based fusion is superior to FSVB-IMM and CS model algorithm by analyzing RMSE and alarm condition after typical ADS-B failure modes injected. In some conditions, although the ADS-B information deteriorates, the fusion system can ensure the normal operation, which reduces the probability of system failure. Those are the positive gains brought by fusion. Next it's necessary to improve TCAS and ADS-B system failure library, consider the implicit failure caused by information fusion and propose solutions of locating the failure source reversely.

ACKNOWLEDGMENTS

This work was supported by National Program on Key Basic Research Project (2014CB744903), National Natural Science Foundation of China (61673270), Shanghai Pujiang Program (16PJD028).

REFERENCES

[1] Lin, C. E., Li, C. C., Tai, S. F., Tsai, C. F., Chiang, S. C., "Collision avoidance system for low altitude flights," *Journal of Aeronautics, Astronautics and Aviation*, Vol.41, No.3, 2009, pp.143-155.

[2] Da Silva, J. L., Brancalion, J. F., & Fernandes, D, "Data fusion techniques applied to scenarios including ADS-B and radar sensors for air traffic control," *12th International Conference on Information Fusion*, Seattle,WA,USA, July 6, 2009.

[3] HE,G., & XU,Y, "Hybrid surveillance and collision avoidance system based on TCAS II and ADS-B," *Electric and control*, Vol.18, No.4, 2011, pp.61-64.

[4] Peng, L. F., Lin, Y. S., & Huang, Q. Z, "Scheme design of collision avoidance system for formation flight based on SSR and ADS-B hybrid surveillance," *Journal of telecommunications technology*, Vol.52, No.5, 2012, pp.609-614.

[5] Sabatini, R., Gardi, A., "A laser obstacle warning and avoidance system for unmanned aircraft sense-and-avoid," *Applied Mechanics and Materials*, Vol.629, 2014, pp.355-360.

[6] Chen, R. H., Gevorkian, A., "Multi-sensor data integration for autonomous sense and avoid," *AIAA Infotech at Aerospace Technical Conference*. 2011.

[7] Mazor, E., Averbuch, A., Bar-Shalom, Y., & Dayan, J, "Interacting multiple model methods in target tracking: a survey," *IEEE Transactions on Aerospace and Electronic Systems*, Vol.34, No.1, 1998, pp.103-123.

[8] Lu, Y., Liu, C., & Liu, P, "An improved tracking method based on data mining in ADS-B for surface surveillance," *2012 9th International Conference on Fuzzy Systems and Knowledge Discovery*. IEEE, 2012, pp.1466-1470.

[9] Chamlou, R., Love, W. D., "Exploration of new algorithms for airborne collision detection and avoidance to meet Next Gen capabilities," *27th Digital Avionics Systems Conference*. IEEE, 2008.

[10] Gao, X., Chen, J., "Multi-Sensor Centralized Fusion without Measurement Noise Covariance by Variational Bayesian Approximation," *IEEE Transactions on Aerospace and Electronic Systems*, Vol.47, No.1, 2011, pp.718-272.

[11] Sarkka, S., & Nummenmaa, A, "Recursive Noise Adaptive Kalman Filtering by Variational Bayesian Approximations," *IEEE Transactions on Automatic Control*, Vol.54, No.3, 2009, pp.596-600.

[12] Ali, B. S., Ochieng, W., Majumdar, A., "ADS-B System Failure Modes and Models," *Journal of Navigation*, Vol. 67, No.06, 2014, pp.995-1017.

[13] Busyairah Syd Ali, *A Safety Assessment Framework for Automatic Dependent Surveillance Broadcast (ADS-B) and its Potential Impact on Aviation Safety*, Doctor Thesis, Transport Studies Department of Civil and Environmental Engineering, Imperial College London, 2013.

[14] Fu, X., Jia, Y., Du, J., & Yu, F, "New interacting multiple model algorithms for the tracking of the manoeuvring target," *IET Control Theory & Applications*, Vol.4, No.10, 2010, pp.2184-2194.

[15] ZHOU, H, Maneuvering target tracking, Beijing, National Defense Industry Press, 1991, pp. 48-70.

[16] LI, B., & WANG, Z, "An improved target tracking algorithm based on the "Current" Statistical Model," *Journal of Projectiles, Rockets, Missiles and Guidance* ,Vol. 28, No.2, 2008, pp.82-83.

[17] Ali B S, Schuster W, Ochieng W, et al. "Framework for ADS-B Performance Assessment: the London TMA Case Study," *Journal of The Institute of Navigation*, Vol.61, No.1, 2014, pp.39-52.

[18] NI Yude, MA Yushen, LIU Ping. "Research on algorithm of ADS-B with TCAS II data fusion," *Computer Engineering and Applications*, Vol.51, No.22, 2015, pp.218-221

[19] Mbalawata, I. S., Särkkä, S., Vihola, M., "Adaptive Metropolis algorithm using variational Bayesian adaptive Kalman filter," *Computational Statistics & Data Analysis*, Vol.83, 2015, pp.101-115.

[20] Bar-Shalom, Y., Challa, S., "IMM estimator versus optimal estimator for hybrid systems," *IEEE Transactions on Aerospace and Electronic Systems*, Vol.41, No.3, 2005, pp. 986-991.

[21] Mallick, M., & La Scala, B. F. "IMM estimator for ground target tracking with variable measurement sampling intervals," *9th International Conference on Information Fusion*. IEEE, 2006, pp.1-8.

[22] Susan J. M. Cabler, "Airworthiness approval of Automatic Dependent Surveillance-Broadcast Out systems," FAA, Washington, July. 2011.

[23] Zili Deng, Optimal estimation theory with application: modeling, filtering, information fusion estimation. Harbin, Harbin Institute of Technology Press, 2005. Chap.6, pp. 377-385.

[24] McCallie, D., Butts, J., & Mills, R, "Security analysis of the ADS-B implementation in the next generation air transportation system," *International Journal of Critical Infrastructure Protection*, Vol.4, No.2, 2011, pp.78-87.

[25] Amirarfaei, F., Baniamerian, A., & Khorasani, K, "Joint kalman filtering and recursive maximum likelihood estimation approaches to fault detection and identification of boeing 747 sensors and actuators," *AIAA Aerospace Science Meeting*, Grapevine, Texas, January 7, 2013.